Qiu, H., Hudson, Z. M., Winnik, M., & Manners, I. (2015). Multidimensional hierarchical self-assembly of amphiphilic cylindrical block comicelles. Science, 347(6228), 1329-1332. DOI: 10.1126/science.1261816

Multidimensional Hierarchical Self-Assembly of Amphiphilic Cylindrical Block Comicelles

Authors: Huibin Qiu,[1] Zachary M. Hudson,[1] Mitchell A. Winnik,[2]* and Ian Manners[1]*

Affiliations:

[1]School of Chemistry, University of Bristol, Bristol, BS8 1TS, United Kingdom

[2] Department of Chemistry, University of Toronto, Toronto, Ontario, M5S 3H6, Canada

*Correspondence to: ian.manners@bristol.ac.uk and mwinnik@chem.utoronto.ca,

Abstract:

Self-assembly of molecular and block copolymer amphiphiles represents a well-established route to micelles with a wide variety of shapes and gel-like phases. We demonstrate an analogous process, but on a longer lengthscale, in which amphiphilic P-H-P and H-P-H cylindrical triblock comicelles with hydrophobic (H) or polar (P) segments that are monodisperse in length are able to self-assemble side-by-side or end-to-end in non-solvents for the central or terminal segments, respectively. This allows the formation of cylindrical supermicelles and 1D or 3D superstructures that persist in both solution and the solid state. These assemblies possess multiple levels of structural hierarchy in combination with existence on a multimicron length scale, features that are generally only found in natural materials.

Main Text:

Amphiphiles such as molecular surfactants and block copolymers have been shown to form a rich variety of self-assembled nanoscopic structures, including spherical micelles, cylinders, nanotubes, bilayers, and vesicles as well as gel-like phases (*1, 2*). The construction of hierarchical colloidal materials on a longer length scale using spherical nanoparticles (*3, 4*), branched nanocrystals (*5*), nanorods (*6*), and nanocubes (*7*) has also recently been the subject of intense investigation. Control over the size, shape and composition of these nanoscopic building blocks has enabled the formation of superstructures with significant structural diversity (*3, 7*). Self-assembly of Janus and patchy nanoparticles formed by surface modification (*8, 9*) or from block copolymers (*10*), including diblock (*11*) and star (*12*) or linear triblock copolymers (*13–15*), has further broadened the range of superstructures that can be prepared. Nevertheless, despite these impressive recent advances, the use of anisotropic amphiphilic building blocks derived from soft-matter remains limited: examples include polymer-based (*16*) and polymer-metal hybrid nanorods (*17, 18*) and self-assembled nanotubes and cylinders (*19, 20*). These approaches

represent the first steps toward the creation of tailored, functional hierarchical structures on the multimicron length scale, a size domain currently dominated by biological assemblies.

We focused on the hierarchical self-assembly of amphiphilic cylindrical P-H-P triblock comicelles, as well as H-P-H triblock comicelles with an inverse sequence of the hydrophobic (H) and polar (P) segments. Their hierarchical self-assembly was controlled by solvent composition by using non-polar, hydrophobic hexane (or decane), and polar, hydrophilic isopropanol (iPrOH). When added alone, these miscible solvents induce the stacking of the P or H segments, respectively. The triblock comicelles were prepared by living crystallization-driven self-assembly (CDSA) in a mixture of hexane and iPrOH (1:3 v/v), a medium in which the comicelles are individually dispersed. Block copolymers with a crystallizable poly(ferrocenyldimethylsilane) (PFS) core-forming block were used as precursors and possessed either a non-polar, corona-forming H block (poly(dimethylsiloxane), PDMS or poly(methylvinylsiloxane), PMVS), or a complementary P block (poly(2-vinylpyridine), P2VP), to form the micelle periphery (Fig. 1, fig. S1). The triblock comicelle building blocks were monodisperse in both the H and P segment lengths, a feature that is characteristic of the living CDSA method (*21–23*).

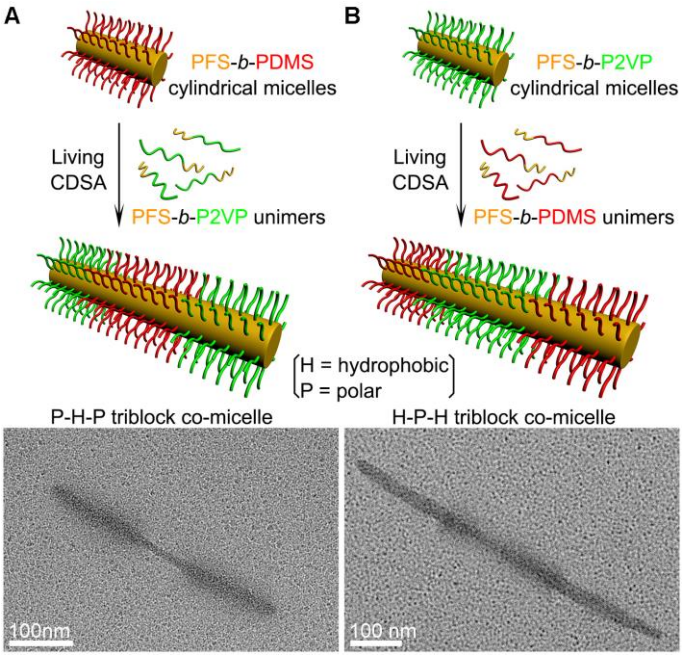

Fig. 1. Formation of amphiphilic cylindrical P-H-P and H-P-H triblock comicelle building blocks via living CDSA. (**A**) P-H-P triblock comicelles with a nonpolar, hydrophobic central segment (H) and two polar terminal segments (P) formed by the addition of PFS_{48}-*b*-$P2VP_{414}$ unimers to a solution of monodisperse cylindrical seed micelles of PFS_{49}-*b*-$PDMS_{504}$. (**B**) H-P-H triblock comicelles with an inverse sequence of the hydrophobic and polar segments formed by the addition of PFS_{49}-*b*-$PDMS_{504}$

unimers to a solution of monodisperse cylindrical seed micelles of PFS_{48}-*b*-$P2VP_{414}$. PDMS corona regions are not visible in the TEM image because of insufficient electron density contrast. The widths of the PFS cores are different for the H and P segments, which is often a feature of living CDSA processes that involve compositionally different block copolymer structures. The PFS core-forming block and the PDMS and P2VP corona-forming blocks are indicated by orange, red and green colors, respectively.

Non-centrosymmetric H-H-P (*24*) and centrosymmetric P-H-P (*25*) amphiphilic triblock comicelles self-assemble in polar media to form spherical supermicelles of size 1 – 5 μm with various aggregation numbers. However, attempts to prepare cylindrical morphologies from P-H-P triblock comicelles by the use of a hydrophobic segment of increased length led only to poorly defined elongated structures (fig. S2). This is likely a result of the use of a terminal P segment with a large degree of polymerization ($P2VP_{414}$) which generates a voluminous hydrophilic corona (overall diameter by TEM in dry state: ca. 70 nm, fig. S3A) that disrupts the stacking of the hydrophobic segments through repulsive interactions (fig. S2C) (*25*). We envisaged that efficient side-by-side stacking of the central core-forming segment of the triblock comicelle is necessary to form well-defined and robust cylindrical structures. Two block copolymers with shorter P2VP blocks: PFS_{34}-*b*-$P2VP_{272}$ and PFS_{20}-*b*-$P2VP_{140}$ were therefore used. The resulting P-H-P triblock comicelles revealed substantially smaller overall terminal P segment diameters by TEM (ca. 40 nm and 20 nm in dry state, respectively: fig. S3), indicating that the corresponding intermicellar steric interactions in supermicelle coronas should be significantly reduced. Indeed, on formation of a polar colloidal solution (hexane : iPrOH 1:3 v/v) of the triblock comicelles $P_{55\ nm}$-$H_{35\ nm}$-$P_{55\ nm}$ (H_h = PFS_{55}-*b*-$PMVS_{825}$, P_p = PFS_{34}-*b*-$P2VP_{272}$ and the subscripts h and p depict the segment length in nm) with a P segment of ca. 40 nm diameter well-defined "train track-like" superstructures were observed by TEM following solvent evaporation due to side-by-side packing (Fig. 2A, fig. S4). The average separation between two parallel triblock comicelles by TEM (corresponding to a low electron density and therefore an invisible region of coronal overlap for the H segments) was found to be ca. 44 nm, slightly larger than the overall diameter of the terminal segments (ca. 40 nm). Longer $P_{80\ nm}$-$H_{55\ nm}$-$P_{80\ nm}$ triblock comicelles with a slightly larger h/p ratio (0.69 vs 0.64) from the same block copolymer constituents were found to afford supermicelles with a significantly tighter packing (average separation = ca. 30 nm) (Fig. 2B). However, to increase the stacking interactions still further to create robust cylindrical architectures we studied the self-assembly of P-H-P (P = PFS_{20}-*b*-$P2VP_{140}$) triblock comicelles with terminal P segments ca. 20 nm in diameter and various segment lengths and h/p ratios in iPrOH. This afforded a variety of well-defined supermicelles of length 1 – 10 μm with a cylindrical morphology (Fig. 2, C-E). Presumably with terminal P segments of even smaller diameter the steric repulsions are further reduced and the central H segments were very tightly stacked, as revealed by an

apparent dark thread by TEM. The formation of persistent cylindrical supermicelles was confirmed by their existence in solution, as demonstrated by optical microscopy in iPrOH (Fig. 2D, Fig. 2E (inset), fig. S5).

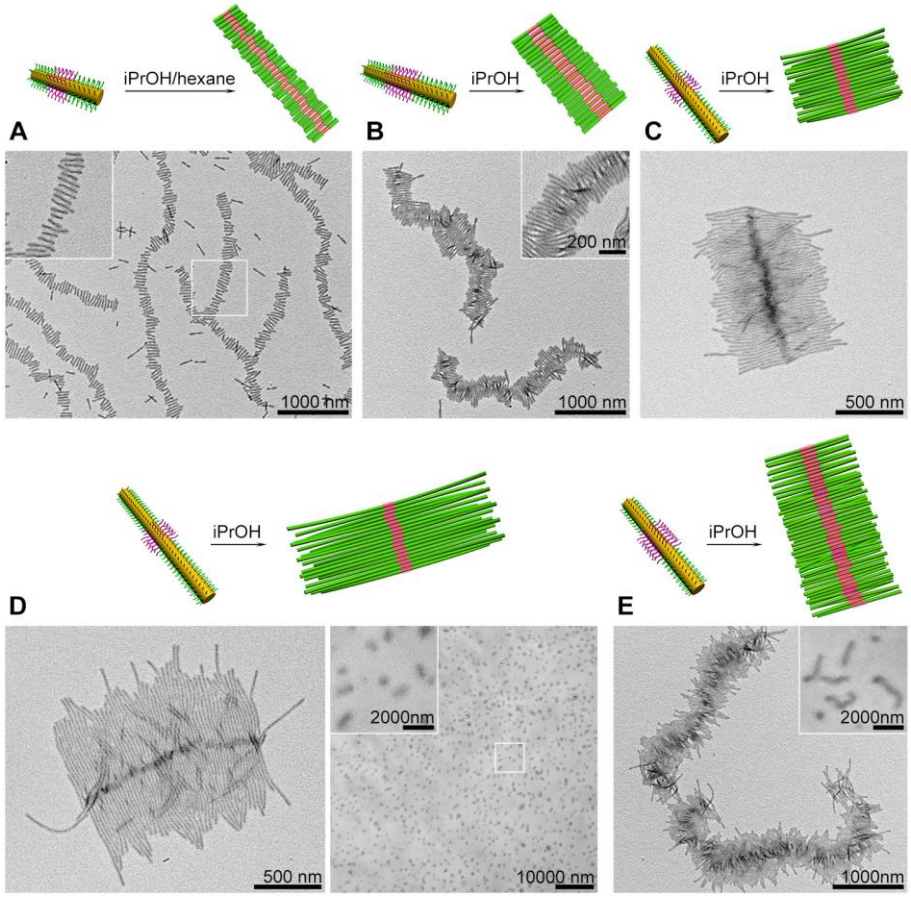

Fig. 2. 1D supermicelles by side-by-side stacking of P-H-P triblock comicelles. (**A**) TEM images of train track-like superstructures formed by $P_{55\ nm}$-$H_{35\ nm}$-$P_{55\ nm}$ (H = PFS_{55}-*b*-$PMVS_{825}$, P = PFS_{34}-*b*-$P2VP_{272}$) triblock comicelles formed on drying from a mixture of hexane and iPrOH (1:3 v/v). (**B**) TEM images of supermicelles with a tighter parallel stacking of $P_{80\ nm}$-$H_{55\ nm}$-$P_{80\ nm}$ (P = PFS_{34}-*b*-$P2VP_{272}$) triblock comicelles formed in iPrOH. (**C**) TEM images of a cylindrical brush-like supermicelle formed by $P_{340\ nm}$-$H_{35\ nm}$-$P_{340\ nm}$ (P = PFS_{20}-*b*-$P2VP_{140}$) triblock comicelles in iPrOH. (**D**) TEM (left) and optical microscopy (right) images of cylindrical brush-like supermicelles formed by $P_{560\ nm}$-$H_{35\ nm}$-$P_{560\ nm}$ (P = PFS_{20}-*b*-$P2VP_{140}$) triblock comicelles formed in iPrOH. (**E**) TEM and optical microscopy (inset) images of longer cylindrical supermicelles formed by $P_{220\ nm}$-$H_{55\ nm}$-$P_{220\ nm}$ (P = PFS_{20}-*b*-$P2VP_{140}$) triblock comicelles in iPrOH. TEM analysis was performed after solvent evaporation. Optical microscopy characterization of the solutions was performed in sealed rectangular capillary tubes. Due to repulsions between the solvated coronas of the P sections, in solution the supermicelles in (**C**) – (**E**) likely take up a

twisted structure in which the parallel stacking of the H sections is slightly compromised rather than the 2D structure revealed by TEM in the dry state.

The formation of multidimensional superstructures by the intermicellar association of terminal segments was also explored using P-H-P triblock comicelles with spatially demanding ca. 70 nm diameter $P2VP_{414}$ coronas for the terminal P segments to favor intermicellar association. To trigger assembly, hexane or decane was rapidly added to a colloidal solution of the triblock comicelles (in 1:3 (v/v) hexane/iPrOH) such that the volume ratio of nonpolar to polar solvent reached 3:1 v/v.

When hexane was used, the end-to-end association yielded discrete superstructures. For the triblock comicelles with relatively short terminal P segments (p = 50 nm) the association predominantly gave irregular loops (e.g. for $P_{50\ nm}$-$H_{260\ nm}$-$P_{50\ nm}$, fig. S7). The terminal segments became fully overlapped at p > 100 nm and the assembly was restricted to a single direction, favoring the formation of linear chain-like superstructures (e.g. for $P_{145\ nm}$-$H_{110\ nm}$-$P_{145\ nm}$, Fig. 3A, fig. S8A). Multiply-stranded chains were formed using more concentrated triblock comicelle solutions (fig. S8A) whereas single-stranded structures resulted when under dilute conditions (Fig. 3A). These chain-like superstructures can be readily made permanent by intermicellar crosslinking of the P2VP coronas of the interacting terminal segments, via coordination of the P2VP pyridyl groups with small Pt nanoparticles (Fig. 3B) (*26, 27*). The ends of the triblock comicelles also remained active towards living CDSA, as demonstrated by the addition of further unimer, enabling the subsequent growth of cylindrical micelle brushes (fig. S10).

Significantly, the degree of end-to-end association dramatically increased when decane was used as the non-polar solvent. This led to an additional level of hierarchical self-assembly, yielding large superstructures that extended in more than one dimension. For example, the triblock comicelles with short terminal segments (p = 50 nm) formed irregular multidimensional architectures in decane (e.g. for $P_{50\ nm}$-$H_{190\ nm}$-$P_{50\ nm}$, Fig. 3C, $P_{50\ nm}$-$H_{110\ nm}$-$P_{50\ nm}$, fig. S11), in which the end-to-end association was random in direction, giving superstructures composed of cross loop-like units. In contrast, the association of micelles with longer terminal segments (e.g. $P_{145\ nm}$-$H_{110\ nm}$-$P_{145\ nm}$) produced disordered superstructures in more concentrated solutions (fig. S8B) but large and continuous networks of chains, with long, multiply-stranded subunits connected by ‘bridging’ micelle chains in dilute solution (Fig. 3D, fig. S12).

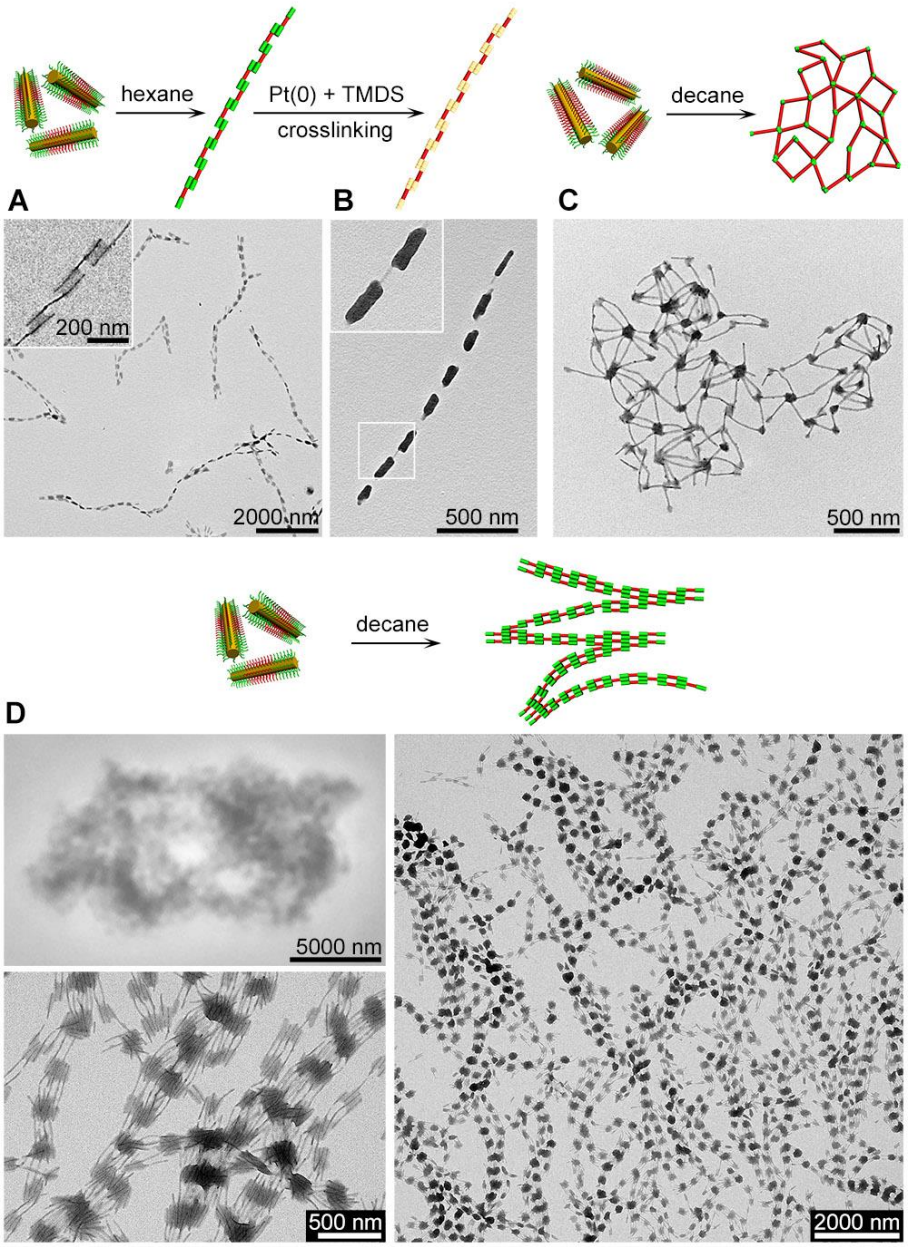

Fig. 3. Multidimensional superstructures by end-to-end stacking of P-H-P triblock comicelles. (**A**) TEM images of mainly single-stranded chains formed by the addition of hexane to a diluted solution (molar concentration = 1/6 original concentration, C_0, see Supplementary Materials for details) of $P_{145\ nm}$-$H_{110\ nm}$-$P_{145\ nm}$ (H = PFS_{49}-*b*-$PDMS_{504}$, P = PFS_{48}-*b*-$P2VP_{414}$) triblock comicelles in 1:3 (v/v) hexane/iPrOH. (**B**) TEM images of an immobilized chain formed by intermicellar crosslinking of P2VP coronas of stacked terminal segments. (**C**) TEM image of an irregular network formed by the addition of decane to a solution (concentration = C_0) of $P_{50\ nm}$-$H_{190\ nm}$-$P_{50\ nm}$ triblock comicelles in 1:3 (v/v) hexane/iPrOH. (**D**) Optical microscopy (top left) and TEM (bottom left and right) images of chain

networks formed by the addition of decane to a diluted solution (concentration = 1/10 C_0) of $P_{145\ nm}$-$H_{110\ nm}$-$P_{145\ nm}$ triblock comicelles in 1:3 (v/v) hexane/iPrOH.

In previous studies (*25*), the nonpolar central H segments of P-H-P triblock comicelles stacked crosswise during the self-assembly in polar media to form spherical supermicelles (fig. S2, A and B). This type of organization for terminal H segments yields higher dimensional assemblies. For example, we found that H-P-H triblock comicelle cylinders (P = PFS_{48}-*b*-$P2VP_{414}$, H = PFS_{49}-*b*-$PDMS_{504}$) self-assemble into a variety of multidimensional superlattices in iPrOH (for H_h-$P_{160\ nm}$-H_h, where h = 70, 105, 250 or 410 nm, Fig. 4, fig. S13). When the terminal segments were relatively short (e.g. h = 105 nm) the H-P-H triblock comicelles preferred to form regular 3D superstructures. TEM analysis revealed dark (electron dense) regions derived from intermicellar association of the H segments and lighter regions with relatively loosely bundled central P segments (see Fig. 4A, fig. S13B). TEM images acquired in a thinner region of the sample showed that the darker dots formed an array with a *d*-spacing of approximately 310 nm (Fig. 4A). Further insight into the organization of the triblock comicelles in the superlattices was revealed by structural reconstruction based on electron tomography (Fig. 4B, fig. S14, movie S1). The darker areas consisting of cross-stacked terminal H segments were woven together by the central P segments across several layers. As the length of the terminal segments was increased the 3D superlattices started to deform and the darker regions began to fuse into strips (e.g. for h = 250 nm, fig. S13C). In contrast, 1D superstructures formed as the length of the terminal H segments was increased to above 400 nm (for h = 410 nm, Fig. 4C, fig. S13D) and the triblock comicelles aligned in a parallel fashion, forming periodically segmented 1D column-like structures. Analogous experiments for triblock comicelle cylinders with a longer central segment (p = 325 nm) revealed similar 3D to 1D structural changes with an increase in the length of the terminal segments ($h \leq 350$ nm for 3D and $h \geq 550$ nm for 1D superlattices) (fig. S15). In this case, values of h/p < ca. 1 favored 3D assemblies while h/p ratios > ca. 1.5 led to a preference for 1D superstructures (Table S4).

To enable direct characterization of the superlattices in solution, green fluorescent dye-labelled PFS_{62}-*b*-($PDMS_{605}$-*r*-G_{21}) (*28*) was blended with PFS_{49}-*b*-$PDMS_{504}$ to form fluorescent hydrophobic terminal segments, H_G (Fig. 4D, Fig. S1). The resulting $(H/H_G)_h$-P_p-$(H/H_G)_h$ (H/H_G = 3:1 by mass) triblock comicelles were readily visualized in solution by confocal laser scanning microscopy (CLSM) (Fig. 4D). Due to the resolution limits of CLSM (fig. S16), we focused on the superlattices formed by the triblock comicelles with longer central segments (p = 570 nm, Fig. 4D, figs. S17, S19). CLSM images (Fig. 4, E and F, figs. S18 and S19, movie S2) clearly showed that the $(H/H_G)_{300\ nm}$-$P_{570\ nm}$-$(H/H_G)_{300\ nm}$ triblock comicelles with h/p ~ 0.5 formed 3D superlattices while the $(H/H_G)_{745\ nm}$-$P_{570\ nm}$-$(H/H_G)_{745\ nm}$ triblock comicelles, with longer terminal segments and h/p ~ 1.3, formed segmented 1D superstructures.

It was also apparent that, in several domains of the 3D superlattices, the fluorescent dots were arranged in a psuedo-rectangular lattice with repeat spacing of ca. 760 nm (Fig. 4E, inset). The use of triblock comicelles with either green- or red fluorescent dye-labeled terminal hydrophobic segments (H_G or H_R) also provided evidence for the lack of micelle building block exchange in solution for both cylindrical supermicelles (fig. S6) and 1D superstructures (fig. S9) over 7 days at 22°C. This indicated that the assemblies formed should be regarded as kinetically-trapped rather than equilibrium structures.

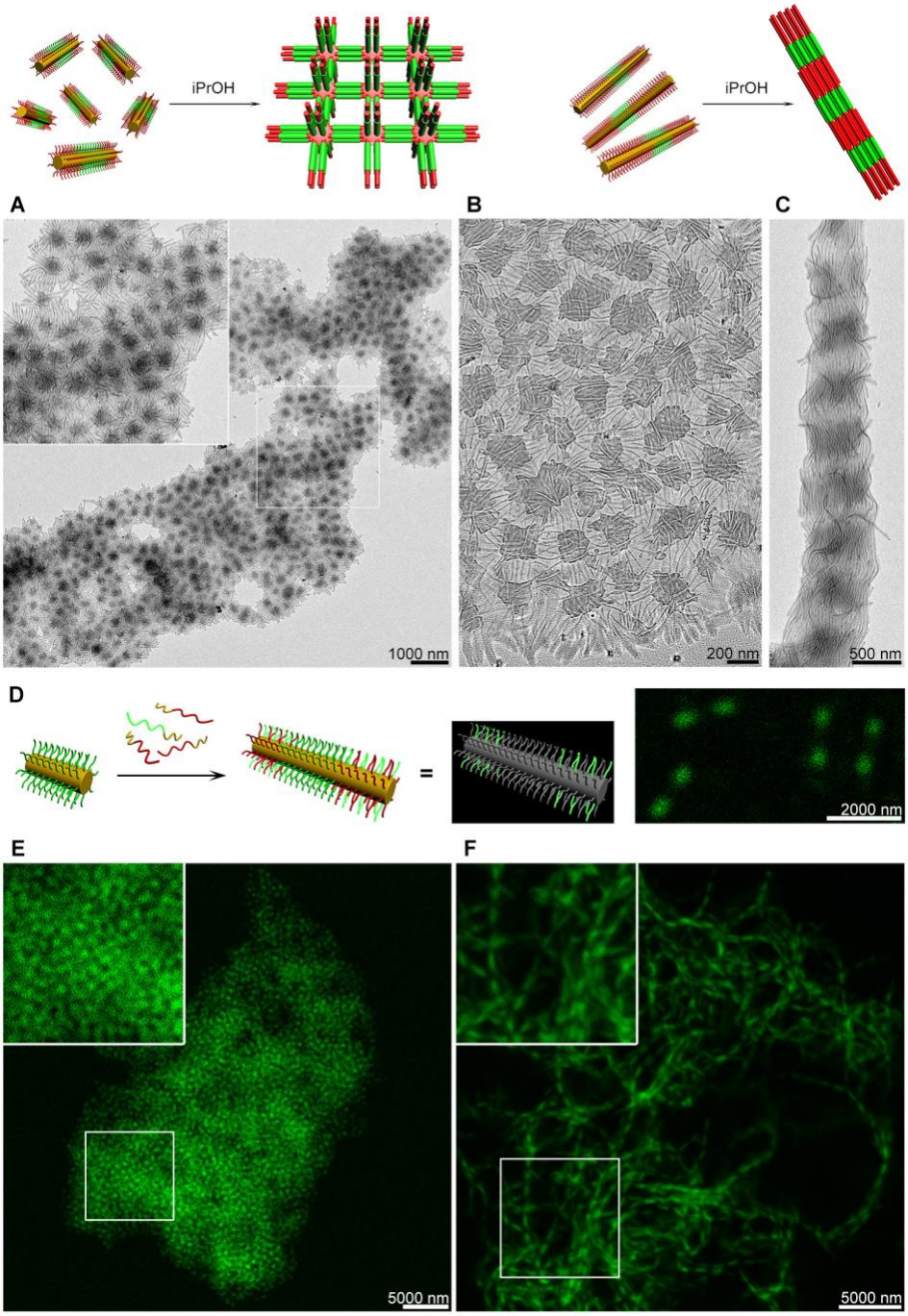

Fig. 4. 3D and 1D superlattices by end-to-end stacking of H-P-H triblock comicelles. (**A**) TEM images of a 3D superlattice formed by $H_{105\ nm}$-$P_{160\ nm}$-$H_{105\ nm}$ (P = PFS_{48}-*b*-$P2VP_{414}$, H = PFS_{49}-*b*-$PDMS_{504}$) triblock comicelles. (**B**) A 3D superlattice revealed by electron tomography and 3D structural reconstruction. (**C**) TEM image of a 1D superlattice formed by $H_{410\ nm}$-$P_{160\ nm}$-$H_{410\ nm}$ triblock comicelles. (**D**) Preparation of fluorescent (H/H_G)-P-(H/H_G) triblock comicelles and CLSM image of $(H/H_G)_{300\ nm}$-$P_{570\ nm}$-$(H/H_G)_{300\ nm}$ triblock comicelles. The fluorescent corona-forming block of PFS_{62}-*b*-($PDMS_{605}$-*r*-G_{21}) is indicated in bright green. (**E**) CLSM images of a 3D superlattice formed by $(H/H_G)_{300\ nm}$-$P_{570\ nm}$-$(H/H_G)_{300\ nm}$ triblock comicelles in iPrOH. (**F**) CLSM images of a 1D superlattice formed by $(H/H_G)_{745\ nm}$-$P_{570\ nm}$-$(H/H_G)_{745\ nm}$ triblock comicelles in iPrOH..

In summary, amphiphilic cylindrical triblock comicelles afford a wide variety of superstructures through side-by-side stacking and end-to-end intermicellar association (Tables S1, S3 and S4). The process is readily controlled by altering the comicelle architecture in terms of the sequence, chemistries, lengths, and diameters of the various segments, as well as the nature of the solvent used. Despite the observation that the self-assembled materials are not formed under equilibrium conditions, the spherical and cylindrical morphologies generated by side-to-side assembly can be qualitatively rationalized through trends in the critical packing parameter, a concept developed for molecular surfactants (Table S2). The formation of 1D or 3D multidimensional structures by end-to-end assembly is related to the h/p ratio where a larger value favors parallel (1D) stacking (Table S4). The coronal blocks can be readily functionalized (as illustrated with fluorescent dyes) and crosslinked; moreover, the CDSA method is applicable to a variety of crystallizable block copolymers (*28*, *29*), including those based on semiconducting (*30*) and biodegradable materials (*31*). The method described therefore offers opportunities to develop functional and robust micron-scale assemblies with potential applications in areas such as sensing, biomedicine, and also in optoelectronics and as photonic crystals.

References and Notes:

1. D. Myer, *Surfactant Science and Technology* (Wiley, New Jersey, ed. 3, 2006).
2. T. Fukino *et al*., Manipulation of discrete nanostructures by selective modulation of noncovalent forces. *Science* **344**, 499-504 (2014).
3. F. Li, D. P. Josephson, A. Stein, Colloidal assembly: the road from particles to colloidal molecules and crystals. *Angew. Chem. Int. Ed*. **50**, 360-388 (2011).
4. I.-H. Lee *et al*., Nanostar and nanonetwork crystals fabricated by in situ nanoparticlization of fully conjugated polythiophene diblock copolymers. *J. Am. Chem. Soc*. **135**, 17695-17698 (2013).

5. K. Miszta *et al*., Hierarchical self-assembly of suspended branched colloidal nanocrystals into superlattice structures. *Nat. Mater*. **10**, 872-876 (2011).

6. T. Wang *et al*., Self-assembled colloidal superlattices from nanorods. *Science* **338**, 358-363 (2012).

7. Z. Quan, J. Fang, Superlattices with non-spherical building blocks. *Nano Today* **5**, 390-411 (2010).

8. Q. Chen, S. C. Bae, S. Granick, Directed self-assembly of a colloidal kagome lattice. *Nature* **469**, 381-384 (2011).

9. Q. Chen *et al*., Supracolloidal reaction kinetics of Janus spheres. *Science* **331**, 199-202 (2011).

10. A. Walther, A. H. E. Müller, Janus particles: synthesis, self-assembly, physical properties, and applications. *Chem. Rev*. **113**, 5194-5261 (2013).

11. K.-Y. Yoon *et al*., One-pot in situ fabrication of stable nanocaterpillars directly from polyacetylene diblock copolymers synthesized by mild ring-opening metathesis polymerization. *J. Am. Chem. Soc*. **134**, 14291-14294 (2012).

12. Z. Li, E. Kesselman, Y. Talmon, M. A. Hillmyer, T. P. Lodge, Multicompartment micelles from ABC miktoarm stars in water. *Science* **306**, 98-101 (2004).

13. H. Cui, Z. Chen, S. Zhong, K. L. Wooley, D. J. Pochan, Block copolymer assembly via kinetic control. *Science* **317**, 647-650 (2007).

14. J. Dupont, G. Liu, ABC triblock copolymer hamburger-like micelles, segmented cylinders, and Janus particles. *Soft Matter* **6**, 3654-3661 (2010).

15. A. H. Gröschel *et al*., Guided hierarchical co-assembly of soft patchy nanoparticles. *Nature* **503**, 247-251 (2013).

16. J.-Y. Wang, Y. Wang, S. S. Sheiko, D. E. Betts, J. M. DeSimone, Tuning multiphase amphiphilic rods to direct self-assembly. *J. Am. Chem. Soc*. **134**, 5801-5806 (2012).

17. K. Liu *et al*., Step-growth polymerization of inorganic nanoparticles. *Science* **329**, 197-200 (2010).

18. Z. Nie *et al*., Self-assembly of metal-polymer analogues of amphiphilic triblock copolymers. *Nat. Mater*. **6**, 609-614 (2007).

19. X. Yan, G. Liu, Z. Li, Preparation and phase segregation of block copolymer nanotube mutiblocks. *J. Am. Chem. Soc*. **126**, 10059-10066 (2004).

20. A. Walther *et al*., Self-assembly of Janus cylinders into hierarchical superstructures. *J. Am. Chem. Soc*. **131**, 4720-3728 (2009).

21. X. Wang *et al*., Cylindrical block copolymer micelles and co-micelles of controlled length and architecture. *Science* **317**, 644-647 (2007).

22. J. B. Gilroy *et al*., Monodisperse cylindrical micelles by crystallization-driven living self-assembly. *Nat. Chem*. **2**, 566-570 (2010).

23. J. Qian *et al*., Self-seeding in one dimension: a route to uniform fiber-like nanostructures from block copolymers with a crystallizable core-forming block. *ACS Nano* **7**, 3754-3766 (2013).

24. P. A. Rupar, L. Chabanne, M. A. Winnik, I. Manners, Non-centrosymmetric cylindrical micelles by unidirectional growth. *Science* **337**, 559-562 (2012).

25. H. Qiu *et al*., Tunable supermicelle architectures from the hierarchical self-assembly of amphiphilic cylindrical B-A-B triblock co-micelles. *Angew. Chem. Int. Ed*. **51**, 11882-11885 (2012).

26. R. K. O'Reilly, C. J. Hawker, K. L. Wooley, Cross-linked block copolymer micelles: functional nanostructures of great potential and versatility. *Chem. Soc. Rev*. **35**, 1068-1083 (2006).

27. H. Qiu, V. A. Du, M. A. Winnik, I. Manners, Branched cylindrical micelles via crystallization-driven self-assembly. *J. Am. Chem. Soc.* **135**, 17739-17742 (2013).

28. Z. M. Hudson, D. J. Lunn, M. A. Winnik, I. Manners, Colour-tunable fluorescent multiblock micelles. *Nat. Commum*. **5**, 3372 (2014).

29. J. Schmelz, A. E. Schedl, C. Steinlein, I. Manners, H. Schmalz, Length control and block-type architectures in worm-like micelles with polyethylene cores. *J. Am. Chem. Soc*. **134**, 14217-14225 (2012).

30. J. Qian *et al*., Uniform, high aspect ratio fiber-like micelles and block co-micelles with crystalline π-conjugated polythiophene core by self-seeding. *J. Am. Chem. Soc*. **136**, 4121-4124 (2014).

31. L. Sun *et al*., Structural reorganization of cylindrical nanoparticles triggered by polylactide stereocomplexation. *Nat. Commum*. **5**, 5746 (2014).

32. Y. Ni, R. Rulkens, I. Manners, Transition metal-based polymers with controlled architectures: well-defined poly(ferrocenylsilane) homopolymers and multiblock copolymers via the living anionic ring-opening polymerization of silicon-bridged [1]ferrocenophane. *J. Am. Chem. Soc.* **118**, 4102-4114 (1996).

33. J. A. Massey *et al*., Self-assembly of organometallic block copolymer: the role of crystallinity of the core-forming polyferrocene block in the micellar morphologies formed by poly(ferrocenylsilane-*b*-dimethylsiloxane) in *n*-alkane solvents. *J. Am. Chem. Soc.* **122**, 11577-11584 (2000).

34. H. Wang, M. A. Winnik, I. Manners, Synthesis and self-assembly of poly(ferrocenyldimethylsilane-*b*-2-vinylpyridine) diblock copolymers. *Macromolecules* **40**, 3784-3789 (2007).

35. X. Wang *et al*., Shell-cross-linked cylindrical polyisoprene-*b*-polyferrocenylsilane (PI-*b*-PFS) Block copolymer micelles: one-dimensional (1D) organometallic nanocylinders. *J. Am. Chem. Soc.* **129**, 5630-5639 (2007).

36. J. N. Israelachvili, D. J. Mitchell, B. W. Ninham, Theory of self-assembly of hydrocarbon amphiphiles into micelles and bilayers. *J. Chem. Soc*., *Faraday Trans*. *2* **72**, 1525-1568 (1976).

37. R. Nagarajan, Molecular packing parameter and surfactant self-assembly: the neglected role of the surfactant tail. *Langmuir* **18**, 31-38 (2002).

Acknowledgments: H.Q. acknowledges the European Union (EU) for a Marie Curie Postdoctoral Fellowship and the ERC for a Postdoctoral Fellowship. Z.M.H. is grateful to the EU for a Marie Curie Postdoctoral Fellowship. I.M. thanks the EU for an ERC Advanced Investigator Grant. M.A.W. thanks the NSERC of Canada for financial support. The authors also thank Judith Mantell and Alan Leard (Wolfson Bioimaging Facility, University of Bristol) for TEM, CLSM and optical microscopy imaging and tomography analysis.

Author contribution: H.Q. and I.M. conceived the project and H.Q. performed the experiments. Z.M.H. prepared the fluorescent PFS block copolymers. H.Q., Z.M.H, and I.M. prepared the manuscript with input from M.A.W. The project was supervised by I.M. with input from M.A.W.

Supplementary Materials:

Materials and Methods

Figures S1-S19

Movies S1-S2

References (*32*-*37*)